ELSEVIER

Journal of Organometallic Chemistry 650 (2002) 25–36

Journal of Organo metallic Chemistry

www.elsevier.com/locate/jorganchem

Synthesis and structural behavior of the P-functional organotin chlorides $[Ph_2P(CH_2)_3]_2SnCl_2$, $Ph_2P(CH_2)_3SnCl_2Me$, and $Ph_2P(CH_2)_nSnCl_3$ ($n = 2$, 3)

Matthias Seibert, Kurt Merzweiler, Christoph Wagner, Horst Weichmann *

Fachbereich Chemie, Institut für Anorganische Chemie, Martin-Luther-Universität Halle-Wittenberg, Kurt-Mothes-Straße 2, D-06120 Halle (Saale), Germany

Received 27 September 2001; accepted 6 December 2001

Abstract

The P-functional organotin dichloride $[Ph_2P(CH_2)_3]_2SnCl_2$ (**3**) is synthesized by reaction of $Ph_2P(CH_2)_3MgCl$ with $SnCl_4$ independently of the molar ratio of the starting compounds. The corresponding organotin trichlorides $Ph_2P(CH_2)_nSnCl_2R$ (**4**: $n = 2$, R = Cl; **5**: $n = 3$, R = Cl; **6**: $n = 3$, R = Me) are formed in a cleavage reaction of $Ph_2P(CH_2)_nSnCy_3$ ($n = 2$, 3) with $SnCl_4$ or $MeSnCl_3$, respectively. The main features of the crystal structures of **3**–**6** are both intra- and intermolecular P···Sn coordinations and the existence of intermolecular Sn–Cl···Sn bridges. For further characterization of the title compounds, the adducts **4**$(Ph_3PO)_2$ (**7**) and **5**(Ph_3PO) (**8**), as well as the P-oxides and P-sulfides of **3**–**6** (**9**–**15**), are synthesized. The results of crystal structure analyses of **7**, **11**, **12**, and **14** are reported. The structures of **9**–**15** are characterized by intramolecular P = X···Sn interactions (X = O, S). A first insight into the structural behavior of the compounds **3**–**15** in solution is discussed on the basis of multinuclear NMR data. © 2002 Elsevier Science B.V. All rights reserved.

Keywords: Organotin; Crystal structure; P–Sn coordination; Hexacoordination; Pentacoordination; NMR spectroscopy

1. Introduction

The P-functional organotin compounds $R_2PCH_2CH_2SnR'_3$ (R, R′ = Me, Ph) and $(Me_2PCH_2CH_2)_2SnMe_2$ have been used as ligands in transition metal complexes. When the transition metal in these complexes is in the usual oxidation state the organotin ligands are coordinated by the phosphorus atom without any interaction between the transition metal and the tin atom [1–3]. Starting complexes with the transition metal in a low-valent state react with the above mentioned P-functional stannanes and also with the distannane $[Ph_2P(CH_2)_2SnMe_2]_2$ in a chelate assisted oxidative addition reaction to give metallacycles with the structural element $\overline{[M]\leftarrow PR_2CH_2CH_2Sn}R'_2$ [4–7].

Recently, we described reactions of the P-functional organotin chloride $Ph_2PCH_2CH_2Sn(Cl)Me_2$ with $[Rh(Cl)(CO)_2]_2$ [8] and various Ni^{II}, Pd^{II}, and Pt^{II} chloride compounds [9]. We obtained complexes in which the tin compound is bonded as a chelate ligand at the transition metal atom by P → [M] coordination and intra- or intermolecular [M]–Cl···Sn bridges. These primary complexes can undergo further reactions, e.g. the complex $[PdCl_2\{PPh_2CH_2CH_2Sn(Cl)Me_2\}_2]$ reacts with sodium amalgam or C_8K under dechlorination to give metallacycles with one or two Sn–Pd bonds [9].

In continuation of these studies we are interested in the use of ω-diphenylphosphinoalkyltin di- and trichlorides with a higher Lewis-acidity of the tin center as ligands in transition metal complexes. In the following paper we describe the synthesis and the structural behavior of $[Ph_2P(CH_2)_3]_2SnCl_2$, $Ph_2P(CH_2)_3SnCl_2Me$, and $Ph_2P(CH_2)_nSnCl_3$ ($n = 2$, 3).

2. Results and discussion

2.1. Synthetic aspects

The preparation of the title compounds by halogenation of the corresponding ω-diphenylphosphinoalkyl methylstannanes $Ph_2P(CH_2)_nSnMe_3$ ($n = 2$, 3) and [Ph$_2$-

---

* Corresponding author. Tel.: + 49-345-5525624; fax: + 49-345-5527028.

E-mail address: weichmann@chemie.uni-halle.de (H. Weichmann).

PII: S0022-328X(02)01116-6

$P(CH_2)_3]_2SnMe_2$ failed because the usual halogenation agents such as halogenes, hydrogen and metal halides attack the phosphorus atom. Efforts to synthesize $Ph_2P(CH_2)_2SnX_2Me$ (X = Br, I) by desulfurization of their sulfides $Ph_2P(S)(CH_2)_2SnX_2Me$ (X = Br, I) with n-Bu_3P or $(Me_2N)_3P$ were also unsuccessful. The sulfides $Ph_2P(S)(CH_2)_2SnX_2Me$ (**1**: X = Br, **2**: X = I) are formed by reaction of $Ph_2P(S)CH_2CH_2SnMe_3$ [10] with Br_2 and I_2, respectively, in CH_2Cl_2 (Eq. (1)).

$$Ph_2P(S)(CH_2)_2SnMe_3 + 2X_2 \xrightarrow{(CH_2Cl_2)} \underset{\mathbf{1}:\ X = Br,\ \mathbf{2}:\ X = I}{Ph_2P(S)(CH_2)_2SnX_2Me} + 2MeX \qquad (1)$$

After removal of the solvent in vacuum and recrystallization of the residue from CH_2Cl_2–n-hexane **1** and **2** are obtained as brownish or colorless crystals, respectively. In both compounds the tin atom is pentacoordinated both in the solid state and in solution as result of an intramolecular P=S···Sn interaction. This is confirmed by the high-field shift of their ^{119}Sn-NMR signals (**1**: − 35.9, **2**: − 198.0 ppm) compared with those of Me_2SnX_2 (X = Br, I; δ_{119Sn}: 70, − 159 ppm, respectively [11]) and the relatively small coupling constants $^nJ(^{119}Sn, ^{31}P)$ ($^nJ(^{119}Sn, ^{31}P) = |^3J(^{119}SnCC^{31}P)| + |^2J(^{119}SnS^{31}P)$ [12,13]) in the ^{31}P and ^{119}Sn-NMR spectra of **1** and **2**. Furthermore, the crystal structure of **2** reveals the existence of discrete monomeric units with a slightly distorted trigonal–bipyramidal ligand polyhedron around the tin atom (d(Sn–I): 2.706(2) (eq), 2.850(2) (ax) Å; d(Sn–S): 2.852(3) Å; ∢ (I–Sn–S): 176.6(8)°) and without any intermolecular Sn–I···Sn interactions [14].

The Grignard compound $Ph_2P(CH_2)_3MgCl$ in THF [15,16] reacts with $SnCl_4$ in toluene independently of the molar ratio of the components to the bis-P-functional tin dichloride $[Ph_2P(CH_2)_3]_2SnCl_2$ (**3**) (Eq. (2)).

$$2Ph_2P(CH_2)_3MgCl + SnCl_4 \xrightarrow{(THF)} \underset{\mathbf{3}}{[Ph_2P(CH_2)_3]_2SnCl_2} + 2MgCl_2 \qquad (2)$$

Although the formation of $Ph_2P(CH_2)_3SnCl_3$ should be the first step in this reaction its isolation failed even in the presence of an excess of $SnCl_4$. Obviously, the chlorine atom in *trans* position to the phosphorus atom in the trigonal–pyramidal ligand polyhedron around the tin atom in the primary product $Ph_2P(CH_2)_3SnCl_3$ (see molecular structure of **5**) is activated by intramolecular P···Sn coordination and its substitution by a second $Ph_2P(CH_2)_3$ group is the favored reaction.

However, the synthesis of the P-functional tin trichlorides $Ph_2P(CH_2)_2SnCl_3$ (**4**), $Ph_2P(CH_2)_3SnCl_3$ (**5**), and $Ph_2P(CH_2)_3SnCl_2Me$ (**6**) is successful by using the classical Kocheshkov redistribution reaction for the preparation of organotin halides [17,18] modified by Jousseaume et al. [19] for functionally substituted organotin trichlorides. For this purpose, the starting compounds $Ph_2P(CH_2)_nSnCy_3$ (n = 2, 3) (synthesized by hydrostannation of $Ph_2P(CH_2)_nCH{=}CH_2$ (n = 0, 1) with Cy_3SnH (Eq. (3)) [14,20]) react with $SnCl_4$ at room temperature in a molar ratio of 1:1 in the solvent mixture of n-heptane–acetonitrile according to Eq. (4) to **4** and **5** which are available as colorless or greenish crystals, respectively. $MeSnCl_3$ reacts with $Ph_2P(CH_2)_3SnCy_3$ at 50 °C in the same way to colorless crystals of $Ph_2P(CH_2)_3SnCl_2Me$ (**6**), but its reaction with $Ph_2P(CH_2)_2SnCy_3$ to give $Ph_2P(CH_2)_2SnCl_2Me$ failed.

$$Ph_2P(CH_2)_nCH{=}CH_2 + Cy_3SnH \xrightarrow{(AIBN)} Ph_2PCH_2CH_2(CH_2)_nSnCy_3 \quad n = 0, 1 \qquad (3)$$

$$Ph_2P(CH_2)_nSnCy_3 + SnCl_3R \xrightarrow[-Cy_3SnCl]{(n\text{-heptane}-CH_3CN)} \underset{\mathbf{4}:\ n=2,\ R=Cl;\ \mathbf{5}:\ n=3,\ R=Cl;\ \mathbf{6}:\ n=3,\ R=Me}{Ph_2P(CH_2)_nSnCl_2R} \qquad (4)$$

The driving force of the reactions according to Eq. (4) is the thermodynamical stability of **4**–**6** as a result of strong P···Sn coordinations and the formation of Sn–Cl···Sn bridges (see structures of **4**–**6**). Obviously, in case of $Ph_2P(CH_2)_2SnCl_2Me$ the Lewis acidity of the tin atom is to weak to stabilize a similar structure as for **4** and consequently the synthesis of $Ph_2P(CH_2)_2SnCl_2Me$ from $MeSnCl_3$ and $Ph_2P(CH_2)_2SnCy_3$ failed.

3–**6** show a moderate stability towards air and moisture. The compounds are soluble in CH_2Cl_2, $CHCl_3$ and in donor solvents but unsoluble in unpolar solvents.

For further characterization of **3**–**6** some derivatives were synthesized.

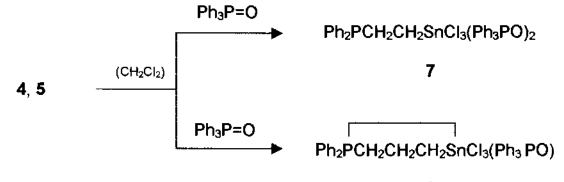

(5)

Owing to the high Lewis acidity of the tin atom in **4** and **5** these compounds react with triphenylphosphine oxide in CH_2Cl_2 according to Eq. (5) to the adducts **7** and **8** which are obtained after evaporation of the reaction solution to dryness and recrystallization of the residue from CH_2Cl_2–n-hexane as colorless crystals.

Furthermore, the diphenylphosphino groups of **3**–**6** were oxidized with NO in acetone and with sulfur in CH_2Cl_2 to the corresponding P-oxides and -sulfides **9**–**15**, respectively (Eqs. (6) and (7)). The oxidation of **3** with NO is incomplete and results in an inhomogeneous product.

$$\mathbf{3} \xrightarrow{sulfur-CH_2Cl_2} \underset{\mathbf{9}}{[Ph_2P(S)CH_2CH_2CH_2]_2SnCl_2} \qquad (6)$$

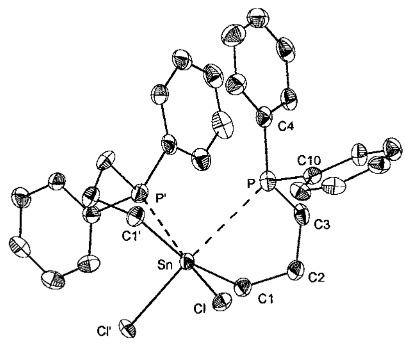

Fig. 1. Molecular structure of $(Ph_2PCH_2CH_2CH_2)_2SnCl_2$ (**3**) with atom-numbering. Hydrogen atoms are omitted for clarity.

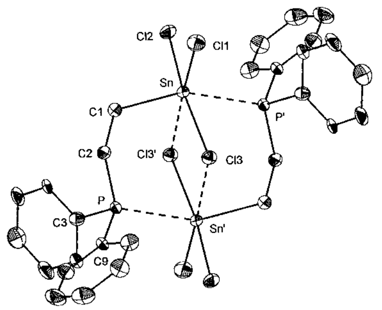

Fig. 2. Molecular structure of $Ph_2PCH_2CH_2SnCl_3$ (**4**) with atom-numbering. Hydrogen atoms and the solvent molecule (CH_2Cl_2) are omitted for clarity.

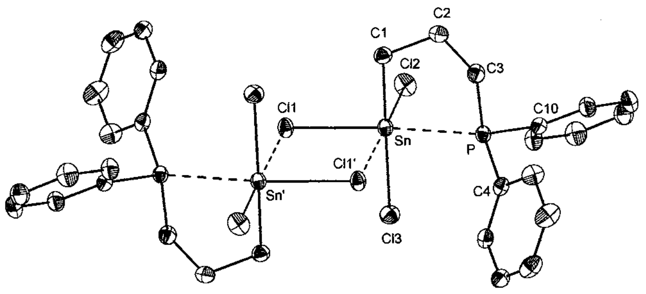

Fig. 3. Molecular structure of $Ph_2PCH_2CH_2CH_2SnCl_3$ (**5**) with atom-numbering. Hydrogen atoms are omitted for clarity.

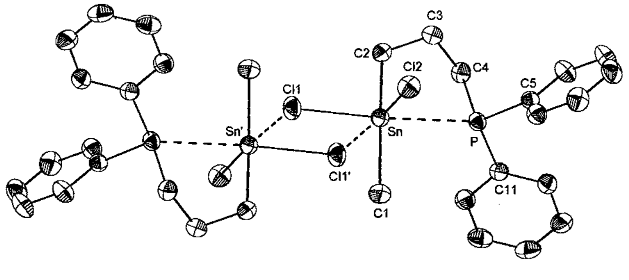

Fig. 4. Molecular structure of $Ph_2PCH_2CH_2CH_2SnCl_2Me$ (**6**) with atom-numbering. Hydrogen atoms are omitted for clarity.

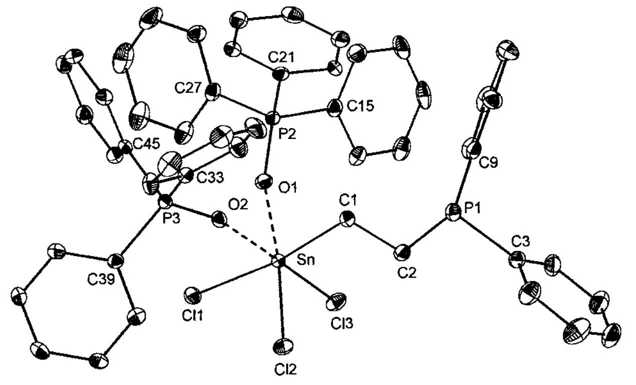

Fig. 5. Molecular structure of $Ph_2PCH_2CH_2SnCl_3(Ph_3PO)_2$ (**7**) with atom-numbering. Hydrogen atoms and the solvent molecule (CH_2Cl_2) are omitted for clarity.

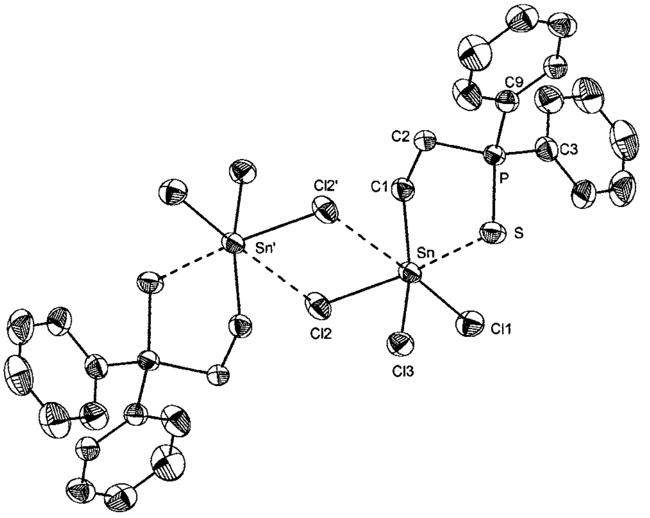

Fig. 6. Molecular structure of $Ph_2P(S)CH_2CH_2SnCl_3$ (**11**) with atom-numbering. Hydrogen atoms are omitted for clarity.

$$\mathbf{4\text{–}6} \xrightarrow[\text{sulfur–CH}_2\text{Cl}_2]{\text{NO–acetone or}} \begin{array}{l} Ph_2P(X)(CH_2)_nSnCl_2R \\ \mathbf{10}\text{: } X = O;\ n = 2;\ R = Cl; \\ \mathbf{11}\text{: } X = S;\ n = 2;\ R = Cl; \\ \mathbf{12}\text{: } X = O;\ n = 3;\ R = Cl; \\ \mathbf{13}\text{: } X = S;\ n = 3;\ R = Cl; \\ \mathbf{14}\text{: } X = O;\ n = 3;\ R = Me; \\ \mathbf{15}\text{: } X = S;\ n = 3;\ R = Me \end{array} \qquad (7)$$

As described for **7** and **8** after working up of the reaction solutions **9**–**15** are obtained as colorless crystals. The compounds are stable under aerobic conditions and are soluble in CH_2Cl_2 and $CHCl_3$.

2.2. Molecular structures of **3**–**6**, **7**, **11**, **12** and **14**

The molecular structures of **3**–**7**, **11**, **12** and **14** are shown in Figs. 1–8 along with the atom-numbering schemes. The crystallographic data are given in Table 7 and selected interatomic parameters are listed in Tables 1–4. All structures are characterized by P···Sn and

$P=X\cdots Sn$ coordinations (X = O, S) and the existence of Sn–Cl···Sn bridges.

The main feature of the structure of **3** is the intramolecular coordination of the phosphorus atom of both diphenylphosphinopropyl groups at the tin atom which becomes thereby hexacoordinated with a distorted octahedral ligand arrangement. The structure includes a twofold axis, which passes through the tin atom. The deviation of the ligand polyhedron around the tin atom from the ideal octahedral geometry is especially apparent in the Cl′–Sn–P and the C1–Sn–C1′ angles of 168.3(1) and 164.0(3)°, respectively, instead of 180°. As found for the most structures of diorganotin dihalides containing two C,Y-chelating ligands (Y = donor atom) [21] in the ligand octahedron at the tin center of **3** the two carbon atoms are in *trans* position and both coordinating phosphorus atoms and the two chlorine atoms are *cis*. The Sn–P distance of 3.086(2) Å is nearly the same as for the P-functional triorganotin chloride $Ph_2P(CH_2)_2Sn(Cl)Me_2$ ($d_{Sn-P}=3.065(3)$ Å [9]) which has a polymeric chain structure attributed to intermolecular P···Sn interactions and the intramolecular coordinated t-$BuPhP(CH_2)_3Sn(Cl)Me_2$ ($d_{Sn-P}=3.078(2)$ Å [22]).

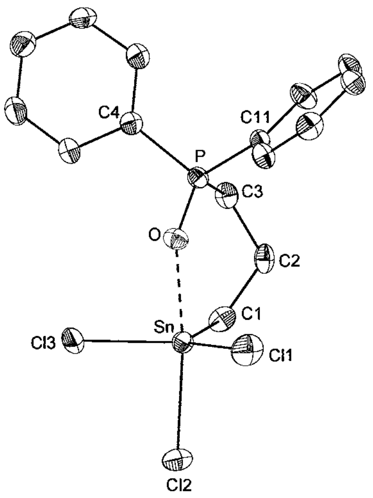

Fig. 7. Molecular structure of $Ph_2P(O)CH_2CH_2CH_2SnCl_3$ (**12**) with atom-numbering. Hydrogen atoms are omitted for clarity.

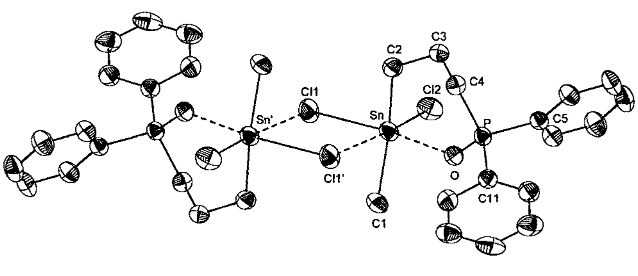

Fig. 8. Molecular structure of $Ph_2P(O)CH_2CH_2CH_2SnCl_2Me$ (**14**) with atom-numbering. Hydrogen atoms are omitted for clarity.

Table 1
Selected bond lengths (Å), angles (°) and endocyclic torsion angles (°) for $[Ph_2P(CH_2)_3]_2SnCl_2$ (**3**) and $Ph_2P(CH_2)_2SnCl_3$ (**4**)

Compound **3**			
Bond lengths			
Sn–Cl	2.487(2)	Sn–C(1)	2.134(6)
Sn–P	3.086(2)		
Bond angles			
Cl–Sn–C(1)	95.6(2)	P–Sn–P′	83.8(1)
Cl–Sn–Cl′	95.9(1)	P–Sn–C(1)′	93.1(2)
Cl–Sn–P	91.0(1)	P–Sn–Cl′	168.3(1)
C(1)–Sn–P	74.9(2)	C(1)–Sn–C(1)′	164.0(3)
C(1)–Sn–Cl′	95.1(2)		
Sn–P–C(3)–C(2)	−35.5(1)		
P–C(3)–C(2)–C(1)	68.7(1)		
C(3)–C(2)–C(1)–Sn	−66.0(1)		
C(2)–C(1)–Sn–P	27.7(1)		
C(1)–Sn–P–C(3)	4.8(1)		
Compound **4**			
Bond lengths			
Sn–Cl(1)	2.389(2)	Sn–Cl(3)′	2.840(3)
Sn–Cl(2)	2.405(2)	Sn–C(1)	2.148(6)
Sn–Cl(3)	2.620(2)	Sn–P′	2.605(2)
Bond angles			
C(1)–Sn–Cl(1)	102.7(2)	P′–Sn–Cl(3)′	77.9(1)
C(1)–Sn–Cl(2)	95.1(1)	Cl(1)–Sn–Cl(2)	93.2(1)
C(1)–Sn–Cl(3)	91.4(1)	Cl(3)–Sn–Cl(3)′	88.3(1)
C(1)–Sn–Cl(3)′	78.0(2)	Cl(2)–Sn–Cl(3)	173.0(1)
P′–Sn–Cl(1)	100.7(1)	C(1)–Sn–P′	154.1(1)
P′–Sn–Cl(2)	94.6(1)	Cl(1)–Sn–Cl(3)′	176.1(1)
P′–Sn–Cl(3)	78.4(1)		

Symmetry transformations used to generate equivalent atoms: **3**: $-x+1$, y, $-z+3/2$; **4**: $-x+1$, $-y$, $-z+2$.

Using the Pauling-type bond order (BO) [23] as a measure for the donor strength of a donor atom X in an intramolecular X···Sn interaction the strength of the P···Sn coordination in **3** (BO = 0.37) is comparable with that of the O···Sn coordination in *cis*-$[MeO(CH_2)_2O(CH_2)_3]_2SnCl_2$ (BO = 0.34) [24], is weaker than the O···Sn interaction in *cis*-$[MeOC(O)CH_2CH_2]_2SnCl_2$ [25] (BO = 0.48) and is considerably weaker than the O···Sn coordination in *cis*-$[H_2NC(O)CH_2CH_2]_2SnCl_2$ [25] (BO = 0.68).

The torsion angles in Table 1 indicate for the two identical five-membered chelate rings in **3** a distorted envelope conformation with the Sn, P, C1 and C3 atoms nearly in a plane.

Compound **4** represents a new structural type in the chemistry of organotin halides. In contrast to $Ph_2P(CH_2)_2Sn(Cl)Me_2$ with an one-dimensional polymeric structure [9] in case of **4** the higher Lewis acidity of the tin atom results in the formation of centrosymmetric dimers by connection of two monomeric units of **4** by Sn–Cl···Sn bridges and the mutual P···Sn coordination of their diphenylphosphinoethyl groups. Fig. 2 shows the tricyclic molecular structure of **4**. The octahedral coordination geometry of the tin atoms in **4** is considerably distorted due to their position as bridgehead atoms in a strained ring system. This is reflected by the small C1–Sn–P′ angle of 154.1(1)° and the difference between the *cis* angles of 77.9(1)–102.7(2)°. Due to the high Lewis acidity of the tin atom in **4** the P···Sn distance of 2.605(2)° is very short and reflects a Pauling type bond order [23] of 0.86 (typical covalent Sn–P bond distance: 2.46 Å [26]). Obviously, as a consequence of the particular steric and electronic situation in the tricyclic ring system of **4** the asymmetry of the internal Sn–Cl···Sn bridges is relatively small ($d_{\text{Sn–Cl3}}$: 2.620(2), $d_{\text{Sn–Cl3}'}$: 2.840(2) Å) and the Sn···Sn distance of 3.85 Å is smaller as the double van der Waals radius of tin (4.34 Å [26]).

Compound **5** and **6** belong to the same structural type (Figs. 3 and 4). In contrast to **4** the length of the propanediyl bridge between the tin and the phosphorus atom allows here an intramolecular P···Sn coordination. Both in **5** and **6** two molecules are connected by Sn–Cl···Sn bridges to centrosymmetric dimers.

Table 2
Selected bond lengths (Å), angles (°) and endocyclic torsion angles (°) for $Ph_2P(CH_2)_3SnCl_3$ (**5**) and $Ph_2P(CH_2)_3Sn(Me)Cl_2$ (**6**)

Compound **5**			
Bond lengths			
Sn–Cl(1)	2.543(1)	Sn–Cl(1)′	2.826(1)
Sn–Cl(2)	2.416(1)	Sn–Cl(3)	2.377(1)
Sn–C(1)	2.153(3)	Sn–P	2.686(1)
Bond angles			
C(1)–Sn–Cl(1)	92.7(1)	Cl(1)–Sn–Cl(2)	95.3(1)
C(1)–Sn–Cl(2)	95.8(1)	Cl(1)–Sn–Cl(1)′	82.4(1)
C(1)–Sn–Cl(1)′	86.4(1)	P–Sn–Cl(2)	100.2(3)
C(1)–Sn–P	82.4(1)	P–Sn–Cl(1)′	82.2(3)
Cl(3)–Sn–Cl(1)	89.6(1)	Cl(1)–Sn–P	164.1(1)
Cl(3)–Sn–Cl(2)	93.4(1)	C(1)–Sn–Cl(3)	170.3(1)
Cl3)–Sn–Cl(1)′	84.6(1)	Cl(2)–Sn–Cl(1)′	177.0(1)
Cl(3)–Sn–P	93.0(1)		
Sn–C(1)–C(2)–C(3)	−57.5(3)		
C(1)–C(2)–C(3)–P	60.3(3)		
C(2)–C(3)–P–Sn	−29.9(2)		
C(3)–P–Sn–C(1)	1.9(1)		
P–Sn–C(1)–C(2)	26.2(2)		
Compound **6**			
Bond lengths			
Sn–Cl(1)	2.516(2)	Sn–P	2.930(2)
Sn–Cl(2)	2.409(1)	Sn–C(1)	2.110(4)
Sn–Cl(1)′	3.385(3)	Sn–C(2)	2.146(3)
Bond angles			
C(1)–Sn–Cl(1)	94.4(1)	P–Sn–Cl(2)	92.9(1)
C(1)–Sn–Cl(2)	104.3(1)	P–Sn–Cl(1)′	88.2(1)
C(1)–Sn–P	90.8(1)	Cl(1)–Sn–Cl(2)	96.1(1)
C(1)–Sn–Cl(1)′	78.7(1)	Cl(1)–Sn–Cl(1)′	82.4(1)
C(2)–Sn–Cl(1)	92.8(1)	C(1)–Sn–C(2)	153.7(2)
C(2)–Sn–Cl(2)	100.0(1)	Cl(1)–Sn–P	168.2(1)
C(2)–Sn–P	78.1(1)	Cl(2)–Sn–Cl(1)′	176.8(1)
C(2)–Sn–Cl(1)′	77.3(1)		
Sn–C(2)–C(3)–C(4)	−58.2(1)		
C(2)–C(3)–C(4)–P	71.6(1)		
C(3)–C(4)–P–Sn	−42.1(1)		
C(4)–P–Sn–C(2)	12.4(1)		
P–Sn–C(2)–C(3)	19.2(1)		

Symmetry transformations used to generate equivalent atoms: **5**: $-x, -y+1, -z+1$; **6**: $-x, -y, -z$.

Table 3
Selected bond lengths (Å), angles (Å) and endocyclic torsion angles (°) for $Ph_2P(CH_2)_2SnCl_3(Ph_3PO)_2$ (**7**) and $Ph_2P(S)(CH_2)_2SnCl_3$ (**11**)

Compound **7**			
Bond lengths			
Sn–C(1)	2.148(4)	Sn–Cl(3)	2.458(1)
Sn–Cl(1)	2.390(1)	Sn–O(1)	2.210(3)
Sn–Cl(2)	2.466(1)	Sn–O(2)	2.201(3)
Bond angles			
C(1)–Sn–O(1)	90.6(1)	O(1)–Sn–O(2)	84.4(1)
C(1)–Sn–O(2)	87.2(1)	O(1)–Sn–Cl(3)	89.9(1)
C(1)–Sn–Cl(2)	92.2(1)	Cl(2)–Sn–O(2)	89.6(1)
C(1)–Sn–Cl(3)	97.4(1)	Cl(2)–Sn–Cl(3)	95.9(1)
Cl(1)–Sn–O(1)	85.0(1)	C(1)–Sn–Cl(1)	171.3(1)
Cl(1)–Sn–O(2)	84.9(1)	O(1)–Sn–Cl(2)	173.2(1)
Cl(1)–Sn–Cl(2)	91.4(1)	O(2)–Sn–Cl(3)	172.6(1)
Cl(1)–Sn–Cl(3)	90.1(1)		
Compound **11**			
Bond lengths			
Sn–Cl(1)	2.379(2)	Sn–Cl(3)	2.353(1)
Sn–Cl(2)	2.507(1)	Sn–C(1)	2.161(3)
Sn–Cl(2)′	3.14(2)	Sn–S	2.621(1)
Bond angles			
C(1)–Sn–Cl(1)	102.2(1)	Cl(1)–Sn–S	95.9(1)
C(1)–Sn–Cl(2)	91.8(1)	Cl(1)–Sn–Cl(2)	95.3(1)
C(1)–Sn–Cl(2)′	78.7(1)	Cl(2)′–Sn–S	87.2(1)
C(1)–Sn–S	89.4(1)	Cl(2)′–Sn–Cl(2)	81.6(1)
Cl(3)–Sn–Cl(1)	98.8(1)	C(1)–Sn–Cl(3)	158.8(1)
Cl(3)–Sn–Cl(2)	89.4(1)	Cl(2)–Sn–S	168.3(1)
Cl(3)–Sn–Cl(2)′	80.5(1)	Cl(1)–Sn–Cl(2)′	176.8(1)
Cl(3)–Sn–S	85.3(1)		
Sn–C(1)–C(2)–P	47.2(1)		
C(1)–C(2)–P–S	−48.6(1)		
C(2)–P–S–Sn	24.5(1)		
P–S–Sn–C(1)	−3.2(1)		
S–Sn–C(1)–C(2)	−23.8(1)		

Symmetry transformations used to generate equivalent atoms: **11**: $-x, -y, -z$.

Compound **5** reveals a new structural motif for organotin trichlorides containing one C,Y-chelating ligand. In all so far published crystal structures of this type of compounds the tin is pentacoordinated by intra or intermolecular coordination of the C,Y-ligand and there are no intermolecular Sn–Cl···Sn interactions [21,27,28].

The structure of **6** is comparable with that of the 1:1 adduct Me_2SnCl_2·diphenylcyclopropenone [29]. The dimeric structures of both compounds with hexacoordinated tin and intermolecular Sn–Cl···Sn bridges are rather untypical because molecular structures both of 1:1 adducts of the type $R_2SnCl_2 \cdot D$ and diorganotin dihalides with one C,Y–chelating ligand in general show pentacoordinated tin without any intermolecular Sn–Cl···Sn contacts [21,30].

The octahedral ligand polyhedron of the tin atom in **5** and **6** is somewhat less distorted than that in the tricyclic ring system of **4**. In contrast to **4** the phosphorus atoms in **5** and **6** are in *trans* position to a chlorine atom due to the intramolecular coordination of the diphenylphosphinopropyl ligand.

In dependence on the Lewis acidity of the tin atom the strength of the P···Sn coordination in **5** (d_{Sn-P}: 2.686(1) Å; BO = 0.77) is comparable with that in **4** whereas that of **6** (d_{Sn-P}: 2.930(2) Å; BO = 0.53) is situated between those of **5** and the organotin monochlorides $Ph_2P(CH_2)_2Sn(Cl)Me_2$ ($d_{Sn-P} = 3.065(3)$ Å; BO = 0.40 [9]) and t-$BuPhP(CH_2)_3Sn(Cl)Me_2$ ($d_{Sn-P} = 3.078(2)$ Å; BO = 0.38 [22]).

Due to the structural difference between the two P-functional tin trichlorides **4** and **5** the latter one shows a greater asymmetry of the Sn–Cl···Sn bridges (**4**: d_{Sn-Cl3}: 2.620(2), $d_{Sn-Cl3'}$: 2.840(2) Å; **5**: d_{Sn-Cl1}: 2.543(1), $d_{Sn-Cl1'}$: 2.826(1) Å). Furthermore, the lower extent of chlorination of the tin atom in **6** results in a further increase of the asymmetry of the Sn–Cl···Sn bridges compared with **5** (**6**: d_{Sn-Cl1}: 2.516(2), $d_{Sn-Cl1'}$: 3.385(3)).

Table 4
Selected bond lengths (Å), angles (°) and endocyclic torsion angles (°) for $Ph_2P(O)(CH_2)_3SnCl_3$ (**12**) and $Ph_2P(O)(CH_2)_3Sn(Me)Cl_2$ (**14**)

Compound **12**			
Bond lengths			
Sn–Cl(1)	2.328(2)	Sn–C(1)	2.128(6)
Sn–Cl(2)	2.453(2)	Sn–O	2.182(5)
Sn–Cl(3)	2.336(2)		
Bond angles			
C(1)–Sn–Cl(1)	121.5(2)	O–Sn–Cl(3)	82.7(1)
C(1)–Sn–Cl(3)	125.2(2)	Cl(2)–Sn–C(1)	96.4(2)
Cl(1)–Sn–Cl(3)	112.1(1)	Cl(2)–Sn–Cl(1)	94.2(1)
O–Sn–C(1)	90.0(2)	Cl(2)–Sn–Cl(3)	90.1(1)
O–Sn–Cl(1)	86.1(1)	O–Sn–Cl(2)	172.3(1)
Sn–O–P–C(3)	9.7(5)		
O–P–C(3)–C(2)	−38.7(5)		
P–C(3)–C(2)–C(1)	74.7(6)		
C(3)–C(2)–C(1)–Sn	−73.4(6)		
C(2)–C(1)–Sn–O	33.3(5)		
C(1)–Sn–O–P	−6.7(4)		
Compound **14**			
Bond lengths			
Sn–C(1)	2.104(8)	Sn–C(2)	2.136(7)
Sn–Cl(1)	2.588(2)	Sn–O	2.227(5)
Sn–Cl(2)	2.408(2)	Sn–Cl(1)′	3.408(1)
Bond angles			
C(1)–Sn–O	83.2(3)	O–Sn–Cl(1)′	90.0(1)
C(1)–Sn–Cl(2)	104.1(3)	O–Sn–Cl(2)	91.4(1)
C(1)–Sn–Cl(1)	91.9(2)	Cl(1)–Sn–Cl(1)′	84.3(1)
C(1)–Sn–Cl(1)′	79.1(1)	Cl(1)–Sn–Cl(2)	94.5(1)
C(2)–Sn–Cl(1)	92.0(2)	Cl(1)–Sn–O	173.2(1)
C(2)–Sn–Cl(1)′	77.7(1)	Cl(2)–Sn–Cl(1)′	176.7(1)
C(2)–Sn–Cl(2)	99.2(2)	C(1)–Sn–C(2)	156.0(4)
C(2)–Sn–O	90.6(2)		
Sn–C(2)–C(3)–C(4)	67.7(1)		
C(2)–C(3)–C(4)–P	−82.7(1)		
C(3)–C(4)–P–O	44.6(1)		
C(4)–P–O–Sn	−2.3(1)		
P–O–Sn–C(2)	−9.0(1)		
O–Sn–C(2)–C(3)	−20.4(1)		

Symmetry transformations used to generate equivalent atoms: **14**: −x, −y, −z.

The torsion angles in Table 2 indicate for the five-membered chelate ring in the molecular structure of **5** a slightly distorted envelope conformation with the C1, Sn, P and C3 atom nearly in a plane. **6** exhibits a conformation between envelope and twist.

The tin atom in the molecular structure of the adduct **7** (Fig. 5) shows the expected octahedral ligand environment. The functional diphenylphosphinoethyl ligand gives rise to some differences in the structures of **7** and the likewise octahedral adduct $EtSnCl_3(Ph_3PO)_2$ [31]. In the latter compound the two P=O groups are in *trans* position whereas these groups are *cis* in compound **7**. Furthermore, in **7** the Sn–O distances (d_{Sn-O}: 2.201(3), 2.210(3) Å) are longer than those in $EtSnCl_3(Ph_3PO)_2$ (d_{Sn-O}: 2.169(5), 2.181(5) Å) and the Sn–Cl bonds *trans* to P=O in **7** are shorter (d_{Sn-Cl}: 2.458(1), 2.466(1) Å) than the two mutual trans standing Sn–Cl bonds in $EtSnCl_3$ $(Ph_3PO)_2$ (d_{Sn-Cl}: 2.487(2), 2.497(2)). This indicates a little stronger *trans* effect for Cl compared with the P=O group in Ph_3PO. The comparison of the values of the angles between the ligands at the tin atom shows the octahedral ligand polyhedron in **7** is somewhat more distorted than in $EtSnCl_3(Ph_3PO)_2$.

The sulfurization of the phosphorus atom in **4** forming compound **11** gives rise to the formation of a five-membered chelate ring due to an intramolecular P=S···Sn interaction (Fig. 6). The ring shows an envelope conformation with the P, S, Sn and C1 atoms nearly in a plane and is puckered at the C2 edge. The Sn–Cl···Sn bridges in **4** remain in existence also in **11**.

The same structural type of **11** and **5** allows a comparison of the donor strength of the Ph_2P and the Ph_2P=S group. The similarity of the Pauling type bond orders (BO) [23] of the P···Sn interaction in **5** (d_{Sn-P}: 2.686(1) Å; BO = 0.77) and the S···Sn coordination in **11** (d_{Sn-S}: 2.621(1) Å; BO = 0.78) and of other structural parameters of both compounds indicate a comparable donor strength of the Ph_2P and the Ph_2P=S group.

In dependence on the Lewis acidity of the tin atom the compounds **12** and **14** show different molecular structures. As has been found for other monoorganotin trichlorides containing a C,Y-chelating ligand (C,Y = $CH_2CH_2C(O)OMe$ [25], $CH_2CH_2C(O)Pr$-i [32], $CH_2CH_2CH_2C(O)OEt$ [33]) the molecular structure of **12** (Fig. 7) consists of monomeric units with an intramolecular P = O···Sn coordination forming a trigonal–bipyramidal ligand polyhedron around the tin atom which differs only slightly from an ideal trigonal bipyramid [$\Sigma\sphericalangle Sn_{eq} - \Sigma\sphericalangle Sn_{ax} = 78.1°$ (TBP: 90°, tetrahedron: 0° [34,35]); Δ (plane) = 0.143(1) Å (TBP: 0 Å, tetrahedron: 0.71 Å [35])]. As expected the P=O group

Table 5
^{119}Sn and ^{31}P-NMR data of **3**–**6**

Compound	$\delta(^{119}Sn)$ (ppm)	$\delta(^{31}P)$ (ppm)	$J(^{119}Sn, ^{31}P)$ (Hz)	Solvent
3	−130 (vb)	−29.0	743	CD_2Cl_2
	−280 (b)	−17.9	57	py-d_5
4	−69 (vb)	14.6 (vb)	–[a]	CD_2Cl_2
	−415 (d, b)	−10.2	720	py-d_5
5	−222 (b)	−32.8	1167	CD_2Cl_2
	−413 (b)	−16.6	<15	py-d_5
6	−26 (d)	−30.3	715	CD_2Cl_2
	−278 (b)	−17.4	19	py-d_5
n-Bu_2SnCl_2 [36]	126.3			$CDCl_3$
	−223			hmpt
n-$BuSnCl_3$ [37]	6			$CDCl_3$
	−457			DMSO-d_6
$Me_2(Cl)Sn(CH_2)_2PPh_2$ [38]	147 (d)	−11.3	171	$CDCl_3$
	−15 (d)	−12.3	267	py-d_5
$Me_2(Cl)Sn(CH_2)_3PPh_2$ [38]	56 (d)	−29.1	234	$CDCl_3$
	−13 (s)	−17.8	<15	py-d_5

Abbreviations: hmpt = hexamethylphosphoric triamide, (b) = broad, (vb) = very broad, (d) = doublet.
[a] Immeasurable because of broadeness.

in **12** is a considerably stronger donor than the C=O group in $EtOC(O)(CH_2)_3SnCl_3$ [33] ($d_{Sn–O}$ (**12**): 2.182(5) Å; BO = 0.82; $d_{Sn–O}$ ($EtOC(O)(CH_2)_3SnCl_3$): 2.405(8) Å; BO = 0.60). The six-membered chelate ring in the molecular structure of **12** is close to an half-boat conformation with the C2 atom to be out of the plane.

The molecular structure of **14** (Fig. 8) is of the same type as those of **5**, **6**, and **11**. The deviation of the ligand octahedron around the tin atom in **14** from the ideal geometry is comparable with that in these compounds. The Sn–O bond length of 2.227(5) Å corresponds to a Pauling bond order of 0.77 which is lower than that in **12** ($BO_{d(Sn–O)} = 0.82$), due to the smaller Lewis acidity of the tin atom in **14**. The six-membered chelate ring in the molecular structure of **14** shows a distorted half-boat conformation with the C3 atom to be out of the plane.

*2.3. NMR investigations of **3**–**15** in solution*

The ^{119}Sn and ^{31}P-NMR data of **3**–**6** and some reference substances in Table 5 allow a rough insight into the behavior of **3**–**6** in CD_2Cl_2 and pyridine-d_5. A comparison of the ^{119}Sn-NMR chemical shifts of **3**–**6** in pyridine with those of n-Bu_2SnCl_2 in hexamethylphosphoric triamide (hmpt) [36] and n-$BuSnCl_3$ in DMSO [37] indicates hexacoordination of the tin atom in all compounds by coordination of two external donor solvent molecules. Accordingly, **3**–**6** form in pyridine the adducts $[Ph_2P(CH_2)_3]_2SnCl_2py_2$ and $Ph_2P(CH_2)_n$-$SnCl_2Rpy_2$ (R = Cl, Me; n = 2, 3), respectively. The open-chained structure of these compounds follows from the considerable difference of the J(Sn, P) coupling constant for **3**, **5**, and **6** in pyridine and in CD_2Cl_2. In pyridine J(Sn, P) is a ^4J(SnCCCP) coupling constant with the expected small value, whereas in CD_2Cl_2 J(Sn, P) as a result of the intramolecular P···Sn coordination is the sum of the contributions $|^1J(SnP)|$ and $|^4J(SnCCCP)|$ [12,13]. Obviously, the considerable contribution of ^1J(Sn P) gives rise to the high values of J(Sn, P) of **3**, **5**, and **6** in CD_2Cl_2.

The considerable upfield shift of the ^{119}Sn-NMR signals of **3**–**6** in CD_2Cl_2 compared with those of n-Bu_2SnCl_2 and n-$BuSnCl_3$ in $CDCl_3$ point to hypercoordinated tin in **3**–**6** also in non-coordinating solvents [36,37,39].

The δ^{119}Sn value of −130 ppm in comparison with n-Bu_2SnCl_2 (δ^{119}Sn = 126 ppm [36]) and the high J(Sn, P) coupling constant of 743 Hz in the spectra of **3** indicate that also in CD_2Cl_2 the PPh_2 group of both functional substituents is intramolecularly coordinated at tin. This is also confirmed by the ^{13}C-NMR spectrum of **3** in CD_2Cl_2 which displays a triplet signal of the $\underline{C}H_2SnCl_2$ carbon atom due to the coupling ^2J(CSnP) with the two Ph_2P groups and the high value of the ^1J(CSn) coupling constant of this carbon atom of 691 Hz indicating hexacoordinated tin [36,40].

The relatively small ^{119}Sn-NMR high-field shift of **4** in CD_2Cl_2 compared with n-$BuSnCl_3$ in $CDCl_3$ ($\Delta\delta^{119}$Sn = −75 ppm), the very large line width both of the ^{119}Sn and the ^{31}P-NMR signal and the strong concentration dependence of these NMR data in this solvent point to an equilibrium between monomeric **4** and its oligomers or polymers with intermolecular P···Sn interactions which is significantly shifted to the side of the monomer (see also [9,38]).

The δ^{119}Sn high-field shift of **5** in CD_2Cl_2 compared with n-$BuSnCl_3$ in $CDCl_3$ ($\Delta\delta^{119}$Sn = −228 ppm) and of **6** compared with n-Bu_2SnCl_2 in $CDCl_3$ ($\Delta\delta^{119}$Sn = −152 ppm) as well as the high values of the J(Sn, P) coupling constants (1167 and 715 Hz) indicate both for **5** and **6** in CD_2Cl_2 a structure with pentacoordinated tin by intramolecular P···Sn coordination [36,37].

With exception of **6** which shows a relatively sharp doublet signal the ^{119}Sn-NMR signals of **3**–**5** in CD_2Cl_2 at room temperature are very broad and without any structure. Furthermore, the chemical shift, the line width and the pattern of the ^{119}Sn and partly also of the ^{31}P-NMR signals of **3**–**6** in CD_2Cl_2 are dependent on temperature and solution concentration. These findings indicate for **3**–**6** dynamic behavior in non-coordinating solvents caused by intra or intermolecular P···Sn dissociation–association processes and/or by stereoisomerizations at the hypercoordinated tin centers. So, the very broad signal in the ^{119}Sn-NMR spectrum of **3** in CD_2Cl_2 at room temperature changes at −60 °C to at least two signal groups with triplet pattern at −290 ppm. This point to the existence of stereoisomers.

In Table 6, the ^{119}Sn and ^{31}P-NMR data of the derivatives **7**–**15** of the title compounds **3**–**6** and some reference substances in CD_2Cl_2 are summarized. For the Ph_3PO adducts **7** and **8** they indicate different structures. In CD_2Cl_2 both adducts undergo a dissociation–association process. As a consequence the ^{119}Sn-NMR spectrum of **7** shows at room temperature no signal. But, at −60 °C three signal groups appear at −505 ppm. One of them is splitted to doublet-to-doublets-to-doublets (^3J(Sn, P) = 756, ^2J(SnOP) = 231 and 99 Hz) and is assigned to one of the three stereoisomers of **7** with two non-equivalent Ph_3PO groups [43]. Whereas **4** coordinates two Ph_3PO molecules giving **7** the strong intramolecular P···Sn coordination in **5** allows only the formation of the 1:1 adduct **8** indicated by the high value of the J(Sn, P) constant which is the same as that of **5** in CD_2Cl_2 (Table 5).

The ^{119}Sn and ^{31}P-NMR data of **9**–**15** correspond to their postulated cyclic structures caused by intramolecular P=X···Sn (X = O, S) interactions forming five and six-membered chelate rings (Figs. 6–8). As expected the P=O···Sn coordination is stronger than the P=S···Sn coordination, documented by the high-field shift of the ^{119}Sn-NMR signals of **10**, **12**, and **14** compared with those of their analogous P=S compounds **11**, **13**, and **15**. The values of the J(Sn, P) coupling constants of **9**–**15** can be interpreted taking into account that they consist of the two contributions $|^nJ(\mathrm{SnC}_m\mathrm{P})|$ ($n = 3$, $m = 2$; $n = 4$, $m = 3$) and $|^2J(\mathrm{SnXP})|$ (X = O, S) and that they depend on the degree of chlorination of the tin atom (see above). As already mentioned above for **3**–**8** the ^{119}Sn signals of **9**–**15** in CD_2Cl_2 at room temperature are broad or broadened, respectively, as a result of dynamic processes which depend on temperature and solution concentrations.

Detailed investigations of the behavior of **3**–**15** in solution are in progress.

3. Experimental

All manipulations were performed under dry argon. Elemental analyses were carried out at the Microanalytical Laboratory of the Chemical Department of the University of Halle. The NMR spectra were recorded on Gemini (200 and 400 MHz) (Varian) or Unity (500 MHz) (Varian) spectrometers. Solvent signals (^{13}C), Me_4Sn (^{119}Sn) and 85% H_3PO_4 (^{31}P) were used as references.

3.1. *$Ph_2P(S)CH_2CH_2SnX_2Me$ (**1**: X = Br; **2**: X = I)*

To a stirred solution of 2 g (4.9 mmol) $Ph_2P(S)CH_2CH_2SnMe_3$ [10] in 30 ml CH_2Cl_2 at −78 °C 1.6 g (20 mmol) bromine or 2.6 g (20.5 mmol) iodine, respectively, are added each dissolved in 10 ml

Table 6
^{119}Sn and ^{31}P-NMR data of **7**–**16** in CD_2Cl_2

Compound	δ(^{119}Sn) (ppm)	δ(^{31}P) (ppm)	J(^{119}Sn, ^{31}P) (Hz)
7	– [a]	−6.6 (PPh_2), 36 (Ph_3PO)	733
8	−428 (b)	−34.8 (PPh_2), 39.6 (Ph_3PO)	1169
9	−55	44.6	29.3
10	−214 (b)	43.3	302
11	−172 (d, b)	53.7	257
12	−297 (b)	54	120
13	−208 (b)	44.6	10
14	−126	48.5	64.7
15	14	42.7	12.3
$Me_2(Cl)Sn(CH_2)_2P(O)Ph_2$ [41]	11	42.6	41
$Me_2(Cl)Sn(CH_2)_2P(S)Ph_2$ [41]	36.4	48.7	63.1
$Me_2(Cl)Sn(CH_2)_3P(O)Ph_2$ [42]	−42.8	40.1	30
$Me_2(Cl)Sn(CH_2)_3P(S)Ph_2$ [42]	113	39.7	12

Abbreviations: (b) broad, (vb) very broad, (d) doublet.

[a] No signal at room temperature.

CH_2Cl_2. After stirring for 2 h at room temperature (r.t.) the solvent is removed and the residue recrystallized from acetone. **1** (0.9 g, 33.5%) and **2** (1.5 g, 46.5%) are obtained as light-brownish or colorless crystals, respectively; m.p. 64–67 °C (**1**), 94–97 °C (**2**).

1: $C_{15}H_{17}Br_2PSSn$ (538.9): Anal. (Exp./Calc.) C, 32.97/33.44; H, 3.14/3.18; Br, 29.03/29.66%. ^{119}Sn-NMR (CD_2Cl_2): δ −35.9 (d, J(Sn, P) 61 Hz) ppm. ^{31}P-NMR (CD_2Cl_2): δ 67.1 (s, J(P, Sn) 60 Hz) ppm.

2: $C_{15}H_{17}I_2PSSn$ (632.8): Anal. (Exp./Calc.) C, 28.32/28.47; H, 2.69/2.71; I, 39.89/40.11%. ^{119}Sn-NMR (CD_2Cl_2): δ −198.0 (d, J(Sn, P) 73 Hz) ppm. ^{31}P-NMR (CD_2Cl_2): δ 49.0 (s, J(P, Sn) 71 Hz) ppm.

3.2. *($Ph_2PCH_2CH_2CH_2)_2SnCl_2$ (**3**)*

A solution of 80 mmol of the Grignard compound $Ph_2PCH_2CH_2CH_2MgCl$ [15,16] in 200 ml THF is added dropwise and under stirring to a solution of $SnCl_4$ (4.6 ml, 39.4 mmol) in 300 ml toluene. A colorless solid precipitates and the supernatant solution changes to yellow. After stirring for 12 h at r.t. and 4 h at 100 °C the solvent is removed in vacuum and the residue extracted three times each with 50 ml of CH_2Cl_2. After concentration of the combined solutions colorless crystals of **3** are obtained (8.7 g, 34.3%); m.p. 197–200 °C.

$C_{30}H_{32}Cl_2P_2Sn$ (644.1): Anal. (Exp./Calc.) C, 54.85/55.94; H, 5.26/5.01; Cl, 11.39/11.01%. ^{13}C-NMR (CD_2Cl_2): δ 22.2(d, P*C*, ^1J(*C*P) 16.1 Hz); 28.3 (s, C*C*C); 39.6 (t, Sn*C*, ^2J(*C*SnP) 28, ^1J(*C*Sn) 691 Hz) ppm. ^{119}Sn-NMR: (CD_2Cl_2, −60 C): δ −182 (m, b), −290.4 (m) ppm.

3.3. *$Ph_2PCH_2CH_2SnCl_3$ (**4**)*

To a solution of $Ph_2PCH_2CH_2SnCy_3$ [14,20] (20 g, 34.4 mmol) in 50 ml of *n*-pentane under vigorous stirring at r.t. 3.9 ml (33.4 mmol) $SnCl_4$ are dropped. A light-greenish solid precipitates. To the reaction mixture further 100 ml of *n*-pentane and 100 ml of acetonitrile are added whereby the solid is partly dissolved. After stirring for 8–10 h at r.t. and filtration the solid is washed three times each with 20 ml of *n*-pentane and dried. Recrystallization from CH_2Cl_2 gives 5.1 g (33.8%) of **3**, which crystallizes with a half mole of solvent; m.p. 122–127 °C.

$C_{14}H_{14}Cl_3PSn$ (438.3) δ CH_2Cl_2 Anal.: (Exp./Calc.) C, 34.42/34.43; H, 3.14/3.08; Cl, 32.86/33.88%.

3.4. *$Ph_2PCH_2CH_2CH_2SnCl_3$ (**5**)*

As described for compound **4** 20 g (33.6 mmol) of $Ph_2PCH_2CH_2CH_2SnCy_3$ [14,20] in 50 ml of *n*-pentane are reacted with 3.9 ml (33.4 mmol) of $SnCl_4$. A light-greenish solid precipitates immediately. After stirring for 3 h further 100 ml of *n*-pentane and 100 ml acetonitrile are added whereby the solid dissolves. After standing of the reaction mixture for 8–10 h at r.t. the phase of acetonitrile is separated. To remove the formed Cy_3SnCl this phase is extracted three times each with 50 ml of *n*-pentane and afterwards the acetonitrile is completely removed in vacuum. The remaining oil is solved in 50 ml CH_2Cl_2 from which **5** crystallizes as a greenish solid (9.3 g, 61.2%); m.p. 144–150 °C.

$C_{15}H_{16}Cl_3PSn$ (452.3) Anal.: (Exp./Calc.) C, 39.46/39.83; H, 3.68/3.57; Cl, 23.28/23.51%. ^{13}C-NMR (CD_2Cl_2, −60 °C): δ 19.7(s, b, *C*P); 23.5 (d, b, C*C*C, J(*C*, P) 12.1 Hz); 36.0 (d, b, *C*Sn, J(*C*, P) 48.9 Hz) ppm. ^{119}Sn-NMR (CD_2Cl_2, −90 °C): δ −228 (m), −404 (m) ppm.

3.5. *$Ph_2PCH_2CH_2CH_2SnCl_2Me$ (**6**)*

A solution of 8 g (33.3 mmol) of $MeSnCl_3$ in 30 ml of *n*-pentane is slowly dropped at r.t. and under vigorous stirring to a solution of 20 g (33.6 mmol) of $Ph_2P(CH_2)_3$ $SnCy_3$ [14,20] in 50 ml of *n*-pentane. After the reaction is finished another 100 ml of *n*-pentane and 100 ml of acetonitrile are added. The reaction mixture is standing for 8–10 h at r.t. and afterwards heated for 3 h at 50 °C. The further working up of the clear reaction mixture is performed as described for compound **5**. Compound **6** is obtained as colorless crystals (9.3 g; 64.6%); m.p. 122–127 °C.

$C_{16}H_{19}Cl_2PSn$ (431.9) Anal.: (Exp./Calc.) C, 44.34/44.50; H, 4.42/4.43; Cl, 15.99/16.42%. ^{1}H-NMR (CD_2Cl_2): δ 1.34 (d, 3H, SnCH_3, $^2J(H_3$CSn) 74.6, $^3J(H_3$CSnP) 4.5 Hz); 2.07–2.34 (3 m, 6H, $CH_2CH_2CH_2$); 7.38–7.53 (m, 10H, C_6H_5) ppm. ^{13}C-NMR (CD_2Cl_2): δ 13.6 (d, H_3*C*Sn, J(*C*Sn, P) 32.3, ^1J(*C*Sn) 574 Hz); 22.1 (d, *C*P, J(*C*, P) 14.9, J(*C*, Sn) 43.9 Hz); 28.8 (d, *C*CP, J(*C*, P) 1.7, J(*C*, Sn) 42.2 Hz); 31.7 (d, H_2*C*Sn, J(*C*, P) 31.5, ^1J(*C*Sn) 602 Hz) ppm. ^{119}Sn-NMR (CD_2Cl_2, −60 °C): δ −84 (d, b, J(*Sn*, P) 861 Hz) ppm.

3.6. *$Ph_2PCH_2CH_2SnCl_3(Ph_3PO)_2$ (**7**)*

Compound **4** (0.2 g, 0.46 mmol) and 0.3 g (1.08 mmol) of Ph_3PO are dissolved in 20 ml of CH_2Cl_2. After 2 h the solvent is completely removed and the residue recrystallized from CH_2Cl_2–*n*-hexane to give 0.3 g (66.1%) of **7**; m.p. 178–181 °C.

$C_{50}H_{44}Cl_3O_2P_3Sn$ (994.9) Anal.: Exp./Calc. C, 59.98/60.36; H, 4.79/4.46; Cl, 11.42/ 10.69%. ^{119}Sn-NMR (CD_2Cl_2, −60 °C): δ −498 (m); −505 (ddd, ^3J(Sn, P) 756, ^2J(SnOP) 231, ^2J(SnOP) 99 Hz); 509 (m) ppm.

3.7. *$Ph_2PCH_2CH_2CH_2SnCl_3(Ph_3PO)$ (**8**)*

In the same manner as described for compound **7** from 0.2 g (0.44 mmol) of **5** and 0.15 g (0.54 mmol) of Ph_3PO results 0.25 g (78.1%) of **8**; m.p. 86–91 °C.

Table 7
Crystal data and details of the refinement

	3	**4**	**5**	**6**	**7**	**11**	**12**	**14**
Formula	$C_{30}H_{32}Cl_2P_2Sn$	$C_{14}H_{14}Cl_3PSn\cdot CH_2Cl_2$	$C_{15}H_{16}Cl_3PSn$	$C_{16}H_{19}Cl_2PSn$	$C_{50}H_{44}Cl_3O_2P_3Sn$	$C_{14}H_{14}Cl_3PSSn$	$C_{15}H_{16}Cl_3OPSn$	$C_{16}H_{19}Cl_2OPSn$
Formula weight (g mol^{-1})	644.09	523.19	452.29	431.87	994.80	470.32	468.29	447.87
Crystal system	Monoclinic	Triclinic	Monoclinic	Monoclinic	Monoclinic	Monoclinic	Orthorhombic	Monoclinic
Space group	$C2/c$	$P\bar{1}$	$P2_1/n$	$P2_1/c$	Cc	$P2_1/n$	$F2dd$	$P2_1/c$
Temperature (K)	203(2)	203(2)	200(2)	r.t.	203(2)	r.t.	r.t.	r.t.
Lattice parameters								
a (Å)	15.272(11)	8.642(3)	9.108(2)	9.209(6)	10.266(2)	9.805(2)	9.775(7)	9.7495(9)
b (Å)	12.447(5)	9.713(7)	16.168(5)	18.057(8)	23.007(5)	14.964(15)	18.236(13)	18.1051(19)
c (Å)	15.404(8)	11.767(6)	11.633(3)	11.368(10)	19.663(9)	12.153(4)	39.48(2)	10.9872(14)
α (°)	90	83.51(7)	90	90	90	90	90	
β (°)	96.68(7)	79.99(5)	98.51(2)	109.88(8)	91.32(4)	96.78(3)	90	109.398(10)
γ (°)	90	82.82(7)	90	90	90	90	90	
V (Å^3)	2908(3)	960.9(9)	1694.4(8)	1778(2)	4643(2)	1771(2)	7037(8)	1829.3(3)
Z	4	2	4	4	4	4	16	4
D_{calc} (g cm^{-3})	1.471	1.808	1.773	1.614	1.423	1.764	1.768	1.626
Absorption coefficient (mm^{-1})	1.190	2.101	2.062	1.816	0.865	2.091	1.994	1.772
2θ Range (°)	4.24–49.96	5.5–50.0	4.34–52.22	4.42–52.12	4.10–51.8	4.34–51.86	4.12–52.02	4.42–50.00
hkl-Indices	$-18\leq h\leq 16$	$-10\leq h\leq 10$	$-11\leq h\leq 11$	$-11\leq h\leq 11$	$-12\leq h\leq 12$	$-12\leq h\leq 4$	$0\leq h\leq 12$	$-11\leq h\leq 11$
	$-15\leq k\leq 15$	$-11\leq k\leq 11$	$0\leq k\leq 19$	$0\leq k\leq 22$	$-25\leq k\leq 25$	$0\leq k\leq 18$	$-22\leq k\leq 22$	$0\leq k\leq 21$
	$-17\leq l\leq 17$	$-13\leq l\leq 14$	$-11\leq l\leq 14$	$-14\leq l\leq 14$	$-24\leq l\leq 24$	$0\leq l\leq 14$	$0\leq l\leq 48$	$-8\leq l\leq 13$
Reflections, measured	6024	9023	6956	5620	13 756	4817	2800	6129
Reflections, unique	2452	3456	3343	3484	6631	2700	1842	3219
Reflections, unique [$F_o > 4\sigma(\|F_o\|)$]	1895	3171	3194	3182	6163	2509	1742	2420
R_{int}	0.0881	0.0481	0.0158	0.0672	0.0338	0.0127	0.0150	0.0364
Number of refined parameters	159	204	245	258	700	237	251	231
R_1, wR_2 (all data)	0.0700, 0.1542	0.0451, 0.1150	0.0248, 0.0627	0.0293, 0.0681	0.0290, 0.0620	0.0228, 0.0524	0.0263, 0.0764	0.0797, 0.1744
R_1, wR_2 [$I > 2\sigma(I)$]	0.0529, 0.1420	0.0395, 0.0966	0.0235, 0.0619	0.0254, 0.0656	0.0251, 0.0594	0.0203, 0.0510	0.0235, 0.0694	0.0503, 0.1219
Largest difference peak and hole (e Å^{-3})	1.162, −1.138	1.565, −2.000	0.585, −0.713	0.469, −0.368	0.682, −0.547	0.202, −0.374	0.323, −0.533	1.014, −1.240
Flack parameter					−0.021(13)			

$C_{33}H_{31}Cl_3OP_2Sn$ (730.6) Anal.: Exp./Calc. C, 53.96/54.25; H, 5.02/4.28; Cl, 14.15/14.56%.

3.8. P-oxides of **4**, **5**, and **6** (**10**, **12**, and **14**)

Into a solution of 0.5 g of each of the title compounds **3**–**6** in 30 ml of CH_2Cl_2 at r.t. nitrogen monoxid is passed for 1 h. Afterwards the solvent is completely removed and the colorless oily solids are recrystallized from CH_2Cl_2–*n*-hexane.

10: 0.24 g (46.2%); m.p. 234–238 °C. $C_{14}H_{14}Cl_3OPSn$ (454.3) Anal.: (Exp./Calc.) C, 36.91/37.02; H, 3.02/3.11; Cl, 22.97/ 23.41%.

12: 0.33 g (63.5%); m.p. 224–226 °C. $C_{15}H_{16}Cl_3OPSn$ (468.3) Anal.: (Exp./Calc.) C, 38.43/38.47; H, 3.72/3.44; Cl, 21.75/22.71%.

14: 0.4 g (76.9%); m.p. 195–197° C. $C_{16}H_{19}Cl_2OPSn$ (447.9) Anal.: (Exp./Calc.) C, 42.84/42.91; H, 4.90/4.28; Cl, 15.93/15.83%.

3.9. P-sulfides of **3**, **4**, **5**, and **6** (**9**, **11**, **13**, and **15**)

To a solution of 0.5 g of each of the title compounds **3**–**6** in 30 ml of CH_2Cl_2 sulfur is added in a molar ratio of 1:1 (in case of **3** 1:2). After 2 h the solvent of the reaction mixture is removed in vacuum and the residue is recrystallized from CH_2Cl_2–*n*-hexane.

9: 0.4 g (72.7%); m.p. 123–127 °C. $C_{30}H_{32}Cl_2P_2S_2Sn$ (708.3): Anal. (Exp./Calc.) C, 50.13/50.88; H, 4.72/4.55; Cl, 11.00/10.01; S, 8.73/9.05%.

11: 0.45 g (83.3%); m.p. 179–181 °C. $C_{14}H_{14}Cl_3PSSn$ (470.4) Anal.: (Exp./Calc.) C, 34.53/35.75; H, 3.05/3.00; Cl, 21.51/22.61; S 6.88/6.82%.

13: 0.5 g (96.2%); m.p. 124–126 °C. $C_{15}H_{16}Cl_3PSSn$ (484.4) Anal.: (Exp./Calc.) C, 36.89/37.20; H, 3.41/3.33; Cl, 22.75/21.96; S, 6.88/6.62%.

15: 0.47 g (94.4%); m.p. 125–126° C. $C_{16}H_{19}Cl_2PSSn$ (464.0) Anal.: (Exp./Calc.) C, 41.33/41.42; H, 4.18/4.13; Cl, 15.15/15.28; S, 6.82/6.91%.

3.10. Crystallographic studies

Crystal data and details of the data collection and refinement are summarized in Table 7. The data collections were performed on a STOE IPDS diffractometer (**3**, **4**, **7**) and on a STOE STADI-IV diffractometer (**5**, **6**, **11**, **12**, **14**) using Mo–K_α radiation. The structures were solved by direct methods and full-matrix least-squares refinements were performed [44]; all non-hydrogen atoms were refined with anisotropic displacement parameters. For molecular drawings DIAMOND 2.1 [45] was used.

4. Supplementary material

Crystallographic data for the structural analyses have been deposited with the Cambridge Crystallographic Data Center, CCDC nos. for **3**, **4**, **5**, **6**, **7**, **11**, **12**, **14** are 170812, 170813, 170814, 170816, 170815, 170818, 170817, 170819, respectively. Copies of this information may be obtained free of charge from The Director, CCDC, 12 Union Road, Cambridge CB2 1EZ, UK (Fax: +44-1223-336033; e-mail: deposit@ccdc.cam.ac.uk or www: http://www.ccdc.cam.ac.uk).

Acknowledgements

The authors thank the Deutsche Forschungsgemeinschaft for financial support.

References

[1] J. Grobe, R. Martin, Z. Anorg. Allg. Chem. 607 (1992) 146.

[2] J. Grobe, E.M. Reifer, B. Krebs, M. Läge, M. Prill, Z. Anorg. Allg. Chem. 623 (1997) 264.

[3] J. Grobe, E.M. Reifer, B. Krebs, M. Läge, M. Prill, Z. Anorg. Allg. Chem. 626 (2000) 478.

[4] C. Müller, U. Schubert, Chem. Ber. 124 (1991) 2181.

[5] U. Schubert, S. Grubert, U. Schulz, S. Mock, Organometallics 11 (1992) 3163.

[6] U. Schubert, S. Grubert, Organometallics 15 (1996) 4707.

[7] H. Weichmann, J. Organomet. Chem. 238 (1982) C49.

[8] D. Kruber, K. Merzweiler, C. Wagner, H. Weichmann, J. Organomet. Chem. 572 (1999) 117.

[9] U. Baumeister, H. Hartung, A. Krug, K. Merzweiler, T. Schulz, C. Wagner, H. Weichmann, Z. Anorg. Allg. Chem. 626 (2000) 2185.

[10] H. Weichmann, G. Quell, A. Tzschach, Z. Anorg. Allg. Chem. 462 (1980) 7.

[11] E.V. van den Berghe, G.P. van der Kelen, J. Organomet. Chem. 26 (1971) 207.

[12] C. Mügge, H. Weichmann, A. Zschunke, J. Organomet. Chem. 192 (1980) 41.

[13] H. Weichmann, B. Rensch, Z. Anorg. Allg. Chem. 503 (1983) 106.

[14] M. Seibert, Thesis, University of Halle, 2000.

[15] S.O. Grim, R.C. Barth, J. Organomet. Chem. 94 (1975) 327.

[16] E. Arpac, L. Dahlenburg, Z. Naturfosch. 35b (1980) 146.

[17] K.A. Kocheshkov, Chem. Ber. 62 (1929) 996.

[18] K. Moedritzer, Organomet. Chem. Rev. 1 (1966) 179.

[19] B. Jousseaume, M. Lahcini, M.C. Rascle, F. Ribot, C. Sanchez, Organometallics 14 (1995) 685.

[20] T. Schulz, Thesis, University of Halle, 1996.

[21] J.T.B.H. Jastrzebski, G. van Koten, Adv. Organomet. Chem. 35 (1993) 241.

[22] H. Weichmann, J. Meunier-Piret, M. van Meerssche, J. Organomet. Chem. 309 (1986) 267.

[23] (a) U. Kolb, M. Beuter, M. Dräger, Inorg. Chem. 33 (1994) 4522;
(b) M. Dräger, Z. Anorg. Allg. Chem. 423 (1976) 53.

[24] J. Susperregui, M. Bayle, J.M. Léger, G. Déléris, M. Biesemans, R. Willem, M. Kemmer, M. Gielen, J. Organomet. Chem. 545–546 (1997) 559.

[25] P.G. Harrison, T.J. King, M.A. Healy, J. Organomet. Chem. 182 (1979) 17.

[26] M. O'Keefe, N.E. Brese, J. Am. Chem. Soc. 113 (1991) 3226.

[27] P. Jaumier, B. Jousseaume, E.R.T. Tiekink, M. Biesemans, R. Willem, Organometallics 16 (1997) 5124.

[28] M. Biesemans, R. Willem, S. Damoun, P. Geerlings, E.R.T. Tiekink, P. Jaumier, M. Lahcini, B. Jousseaume, Organometallics 17 (1998) 90.

[29] S.W. Ng, C.L. Barnes, M.B. Hossain, D. van der Helm, J.J. Zuckerman, V.G. Kumar Das, J. Am. Chem. Soc. 104 (1982) 5359.

[30] D. Schollmeyer, Thesis, University of Halle, 1989, p. 33.

[31] A.T. Tursina, L.A. Aslanov, S.V. Medvedev, A.V. Yatsenko, Koord. Khim. 11 (1985) 417.

[32] R.A. Howie, E.S. Paterson, J.L. Wardell, J.W. Burley, J. Organomet. Chem. 304 (1986) 301.

[33] R.A. Howie, E.S. Paterson, J.L. Wardell, J.W. Burley, J. Organomet. Chem. 259 (1983) 71.

[34] U. Kolb, M. Dräger, B. Jousseaume, Organometallics 10 (1991) 2737.

[35] M. Dräger, J. Organomet. Chem. 251 (1983) 209.

[36] J. Holeček, M. Nádvorník, K. Handlíř, A. Lyčka, J. Organomet. Chem. 315 (1986) 299.

[37] V. Pejchal, J. Holeček, M. Nádvorník, A. Lyčka, Collect. Czech. Chem. Commun. 60 (1995) 1492.

[38] (a) H. Weichmann, J. Organomet. Chem. 262 (1984) 279;
(b) H. Weichmann, unpublished results.

[39] (a) B. Wrackmeyer, Annu. Rep. NMR Spectrosc. 16 (1985) 73;
(b) B. Wrackmeyer, Annu. Rep. NMR Spectrosc. 38 (1999) 203.

[40] T.N. Mitchell, J. Organomet. Chem. 59 (1973) 189.

[41] T.N. Mitchell, B. Godry, J. Organomet. Chem. 490 (1995) 45.

[42] T.N. Mitchell, B. Godry, J. Organomet. Chem. 516 (1996) 133.

[43] R. Colton, D. Dakternieks, Inorg. Chim. Acta 143 (1988) 151.

[44] G.M. Sheldrick, SHELX-97, Programs for Crystal Structure Determination, Göttingen, 1997.

[45] DIAMOND 2.1, Visuelles Informationssystem für Kristallstrukturen, G. Bergerhoff, K. Brandenburg, Bonn, 2000.